International Communications in Heat and Mass Transfer 38 (2011) 757–766

Contents lists available at ScienceDirect

International Communications in Heat and Mass Transfer

journal homepage: www.elsevier.com/locate/ichmt

An analysis of heat transfer in liver tissue during microwave ablation using single and double slot antenna ☆

P. Keangin, P. Rattanadecho *, T. Wessapan

Research Center of Microwave Utilization in Engineering (R.C.M.E.), Department of Mechanical Engineering, Thammasat University (Rangsit Campus), Pathumthani 12120, Thailand

ARTICLE INFO

Available online 9 April 2011

Keywords:
Double slot antenna
Finite element
Liver tissue
Microwave ablation
Single slot antenna
Temperature distribution

ABSTRACT

Microwave ablation (MWA) is a process that uses the heat from microwave energy to kill cancer cells. MWA is able to focus radiation on the desired areas without damaging the surrounding tissue, entail a control of heating power for appropriate temperature distribution. Slot coaxial antennas are the most popular antennas in MWA because of their small dimensions and low cost to manufacture. To effectively treat liver cancer, these antennas can be used to produce a highly localized specific absorption rate (SAR) and temperature distribution pattern. In this work, the interstitial MWA in liver by single and double slot antennas is carried out. This paper focuses on the influence of antenna type on microwave power absorbed, SAR and temperature distribution. The results show that the maximum SAR and temperature appears in the liver tissue in case of single slot antenna which are higher than those of double slot antenna. However, no clear difference between these two microwave coaxial antenna (MCA) models has been shown, due to the low microwave power input from the MCA during MWA process.

1. Introduction

Liver cancer is a significant worldwide public health issue. The disease has a mortality rate of 100% at 5 years in untreated cases [1] and results in the deaths of more than one million people each year worldwide [2]. Possible treatments for liver cancer are surgical operation, cryosurgery, chemotherapy, radiation therapy and RF ablation [3]. However, the majority of the patients are not candidates for surgical resection due to restrictions, such as multifocal disease, tumor size, and position of tumor to key vessels. Cryosurgery uses one or more cryoprobes, inserted into the patient's body at the desired point for application. A cryofluid, typically liquid nitrogen, flows through the probe's interior to completely freeze and destroy the tumor or benign tissue while minimizing the amount of healthy tissue destruction [4]. However, this technique has disadvantage in particle use, in term of uncertainty. Chemical treatment, where adequate chemical injection is administered into artery supplying cancer tissues, and radiation therapy are mostly used to temporarily relieve the symptoms [3]. RF ablation has been recently introduced to be an effective cure for the liver tissue, but this technique includes difficulty in treating large tumors and the potential for incomplete RF tumor ablation near blood vessels [5].

One promising alternative liver cancer treatment is microwave ablation (MWA), using microwaves. The energy from the microwave frequency waves emitted by the microwave coaxial antenna (MCA) creates heat in the local cancerous tissue cancer without the damaging surrounding tissue. MWA is a minimally invasive modality for the local treatment of solid tumors and can also enhance the effects of certain anticancer drugs [6]. MWA results in a large zone of active heating to the liver tissue. Coaxial-based antennas are extremely important for MWA application because of their low cost and small dimensions. Slot coaxial antennas are the most popular antennas in MWA. For a slot antenna, the outer conductor and the center conductor are soldered at the end of the antenna tip and a ring of metal is cut off the antenna outer conductor to be the antenna slot. Saito et al. [7] presented a design for a double slot antenna that is capable of achieving a higher degree of specific absorption rate (SAR) localization than a standard single slot antenna.

Most previous studies of MWA were mainly focused on SAR and did not consider heat transfer caused an incomplete analysis of the results. While clinical treatment with MWA needs to control the tissue temperature and the lesion generation accurately, in order to ensure cancer cells destruction and to minimize side effects to surrounding tissue and surrounding organs. Therefore, modeling of heat transport is needed in order to completely explain the actual process of MWA within the human tissue. Numerical simulation has been used extensively in the studied of MWA as it offers a fast and economical way to evaluate new hypothetical designs. Moreover, finite element (FE) models can provide users with quick, accurate solutions to multiple systems of differential equations, and as such, are well suited to heat transfer problems like ablation.

In this study, the influence of antenna type on microwave power absorbed, SAR and temperature distribution in liver tissue during

☆ Communicated by W.J. Minkowycz.

* Corresponding author.
E-mail address: ratphadu@engr.tu.ac.th (P. Rattanadecho).

0735-1933/$ – see front matter © 2011 Elsevier Ltd. All rights reserved.
doi:10.1016/j.icheatmasstransfer.2011.03.027

Nomenclature

C	heat capacity of liver tissue (J/kg·°C)
C_b	heat capacity of blood (J/kg·°C)
$\vec{E}$	electric field (V/m)
f	microwave frequency (Hz)
$\vec{H}$	magnetic field (A/m)
$\vec{H}_{\varphi 0}$	excitation magnetic field (A/m)
k	propagation constant (m^{-1})
k_{th}	thermal conductivity of liver tissue (W/m·°C)
k_0	propagation constant of free space (m^{-1})
P	input microwave power (W)
Q_{ext}	external heat source (W/m^3)
Q_{met}	metabolic heat source (W/m^3)
r_{inner}	dielectric inner radius (m)
r_{outer}	dielectric outer radius (m)
T	actual temperature (°C)
T_b	temperature of blood (°C)
t	time (s)
Z	wave impedance in the dielectric of the coaxial cable (Ω)

Greek symbols

ρ	density of liver tissue (kg/m^3)
ρ_b	density of blood (kg/m^3)
λ	wave length (m)
λ_{eff}	effective wave length (m)
ω	angular frequency (rad/s)
ω_b	blood perfusion rate (1/s)
ε_0	permittivity of free space (F/m)
$\varepsilon_r^{'}$	relative permittivity (-)
$\varepsilon_{r,\ liver}^{'}$	relative permittivity of liver tissue (-)
σ_{el}	electric conductivity (S/m)
σ_{liver}	electric conductivity of liver (S/m)
μ	permeability (H/m)
μ_r	relative permeability (-)
ν	speed of light in free space (m/s)

Subscripts

b	blood
eff	effective
el	electric
ext	external
i	initial
inner	inner
liver	liver
met	metabolism
outer	outer
r, z, φ	components of cylindrical coordinates
th	thermal
0	free space

Superscripts

T	temperature

MWA, are investigated systematically. Mathematical models based on coupled equations of electromagnetic wave propagation and bioheat equation are solved by using an axisymetric finite element method (FEM). In order to verify the accuracy of the presented mathematical model of MWA, the resulting data of the single slot MCA is validated against the simulation results, obtained by Yang et al. [8]. The simulated results in this study can be used as a guideline for the practical treatment.

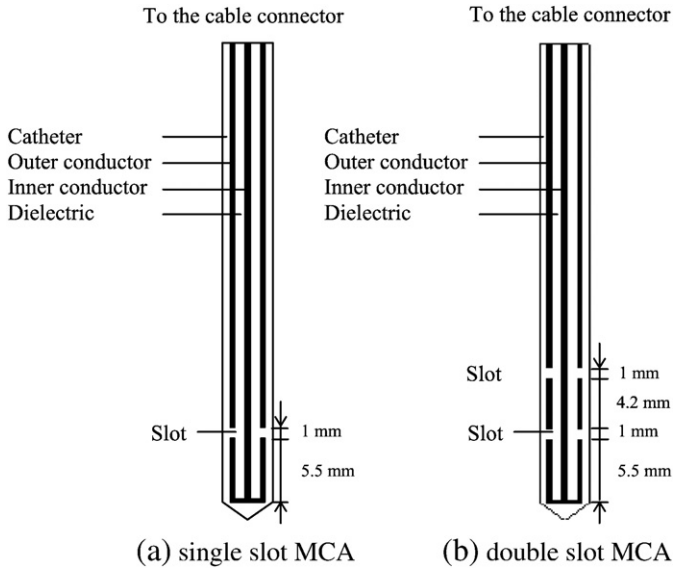

Fig. 1. Model geometry of MCA.

2. Problem statement

This study uses single slot MCA and double slot MCA, to transfer microwave power into liver tissue for the treatment of liver cancer. These antennas have a diameter of 1.79 mm because the thin antenna is required in the interstitial treatments. A ring-shaped slot, 1 mm wide is cut off the outer conductor 5.5 mm in length from the short-circuited tip because the effective heating around the tip of the antenna is very important to the interstitial heating and because the electric field becomes stronger near the slot [7]. The antennas are composed of an inner conductor, a dielectric and an outer conductor. The antennas are enclosed in a catheter (made of polytetrafluorethylene; PTFE), for hygienic and guidance purposes. In case of double slot MCA, the slot spacing are chosen based on the effective wavelength (λ_{eff}) in tissue at frequency of 2.45 GHz, which is calculated using the following equation [9]:

$$\lambda_{eff} = \frac{\nu}{f\sqrt{\varepsilon_r^{'}}} \tag{1}$$

where ν is the speed of light in free space (m/s), f is the operating frequency of the microwave generator (2.45 GHz) and $\varepsilon_r^{'}$ is the relative permittivity of tissue at the operating frequency.

Fig. 1(a) and (b) shows the model geometry of the single slot MCA and double slot MCA, respectively. For the double slot MCA, the slot spacing length of 4.2 mm corresponds to $0.25\lambda_{eff}$. The slot spacing length is chosen to achieve localized power deposition near the distal tip of the antenna.

The MCA operates at the frequency of 2.45 GHz, a widely used frequency in MWA, and the input microwave power is 10 W. The goal

Table 1
Dimensions of a MCA.

Materials	Dimensions (mm)
Inner conductor	0.135 (radial)
Dielectric	0.335 (radial)
Outer conductor	0.460 (radial)
Catheter	0.895 (radial)
Slot	1.000 (wide)

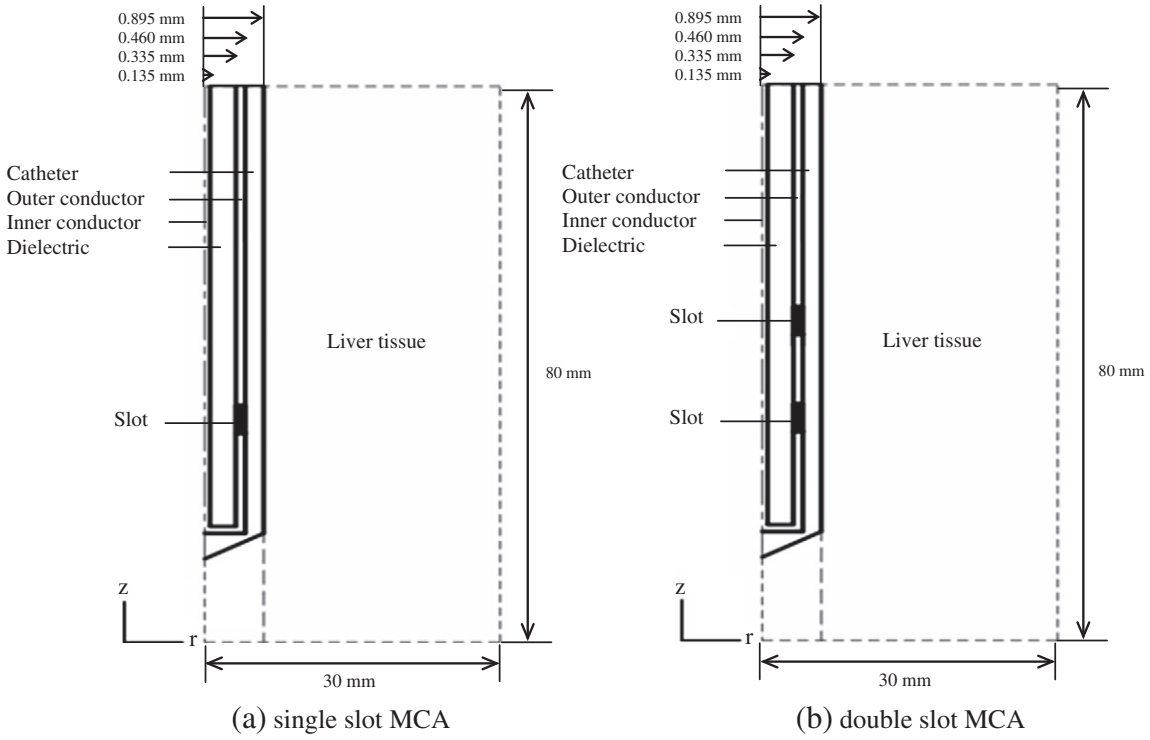

Fig. 2. Axially symmetrical model geometry.

of MWA is to elevate the temperature of un-wanted tissue to 50 °C where cancer cells are destroyed [10]. Dimensions of the MCA are given in Table 1.

The liver tissue is considered as a cylindrical geometry. It has a 30 mm radius and 80 mm in height, and a MCA is inserted into the liver tissue with 70.5 mm depth. An axially symmetric model is considered in this work, which minimized the computation time while maintaining good resolution and the full three-dimensional nature of the fields. The model assumes that the MCA is immersed in a homogeneous smooth biological tissue. The vertical axis is oriented along the longitudinal axis of the MCA, and the horizontal axis is oriented along the radial direction. Fig. 2(a) and (b) shows the mathematical models for MWA in case of using the single slot and double slot, respectively.

The horizontal z axis is oriented along the longitudinal axis of the MCA and the vertical r axis is oriented along the radial direction. The computational domain corresponds to a physical domain size of 30 mm in radius and 80 mm in length, surrounded by air.

The physical properties of the materials involved in the model are selected from several literatures; Yang et al. [8], Bertram et al. [11], Yang et al. [12] and Jacobsen and Stauffer [13]. The properties of liver tissue and MCA are given in Table 2 considered at frequency of 2.45 GHz.

3. The formulation of the mathematical model

A mathematical model has been formulated to predict the microwave power absorbed in the MCA and liver tissue and the temperature distribution in liver tissue under the MWA process. As a rudimentary step of the study, some assumptions are made to simplify the analysis. The liver tissue is the homogeneous biomaterial. In the electromagnetic wave propagation analysis, a scattering boundary condition is set on that surface, which means that the boundary does not disturb the electromagnetic field distribution. The microwave source is set at the upper end of the MCA and the power emitted is adjusted to 10 W. An electromagnetic wave, propagating in a MCA, is characterized by transverse electromagnetic fields (TEM) [11]. In the liver tissue, an electromagnetic wave is characterized by transverse magnetic fields (TM) [11]. The model assumes that the wall of the MCA is a perfect electric conductor, and the dielectric properties of liver tissue have been determined as a function of temperature. While in the heat transfer analysis, temperature dependent properties are considered for the thermal properties. No phase change occurs within the liver tissue, no energy exchange through the outer surface of liver tissue, and no chemical reactions occur within the liver tissue. The outer surface between the MCA and liver tissue is considered as

Table 2
Properties of liver tissue and MCA.

Parameters	Values	Parameters	Values
Properties of liver tissue		Electric conductivity of dielectric; σ_{diel}	0 S/m
Density of blood; ρ_b	1060 kg/m^3	Relative permeability of dielectric; $\mu_{r,\ diel}$	1
Specific heat capacity of blood; C_b	3600 J/kg·°C	Relative permittivity of catheter; $\varepsilon'_{r,\ cat}$	2.1
Blood temperature; T_b	37°C	Electric conductivity of catheter; σ_{cat}	0 S/m
Relative permeability of liver tissue; $\mu_{r,\ liver}$	1	Relative permeability of catheter; $\mu_{r,\ cat}$	1
Metabolic heat source, Q_{met}	33,800 W/m^3	Relative permittivity of slot; $\varepsilon'_{r,\ slot}$	1
Properties of MCA		Electric conductivity of slot; σ_{slot}	0 S/m
Relative permittivity of dielectric; $\varepsilon'_{r,\ diel}$	2.03	Relative permeability of slot; $\mu_{r,\ slot}$	1

adiabatic boundary condition. The relevant boundary conditions are described in Fig. 3.

3.1. Electromagnetic wave propagation analysis

The axisymetric FE model used in this study is adapted from a MCA general model [8,9]. In this model, the electric and magnetic fields associated with the time-varying TEM wave are expressed in 2D axially symmetrical cylindrical coordinates:

$$\text{Electricfield}\left(\vec{E}\right) \qquad \vec{E} = e_r \frac{C}{r} e^{j(\omega t - kz)} \tag{2}$$

$$\text{Magneticfield}\left(\vec{H}\right) \qquad \vec{H} = e_\varphi \frac{C}{rZ} e^{j(\omega t - kz)} \tag{3}$$

where $C = \sqrt{\frac{ZP}{\pi.\ ln(r_{outer}/r_{inner})}}$, Z is the wave impedance, P is the input microwave power (W), r_{inner} is the dielectric inner radius (m), r_{outer} is the dielectric outer radius (m), $\omega = 2\pi f$ is the angular frequency (rad/s), f is the frequency (Hz), $k = \frac{2\pi}{\lambda}$ is the propagation constant (m^{-1}), and λ is the wave length (m).

In the liver tissue, the electric field also has a finite axial component, whereas the magnetic field is purely in the azimuth direction. The electric field is in the radial direction only inside the coaxial cable and in both radial and the axial direction inside the tissue. This allows for the antenna to be modeled using an axisymmetric TM wave formulation. The wave equation then becomes scalar in H_φ:

$$\nabla \times \left(\left(\varepsilon_r' - \frac{j\sigma_{el}}{\omega \varepsilon_0} \right)^{-1} \nabla \times \vec{H}_\varphi \right) - \mu_r k_0^2 \vec{H}_\varphi = 0 \tag{4}$$

where $\varepsilon_0 = 8.8542 \times 10^{-12}$ F/m is the permittivity of free space.

The changes in liver tissue dielectric properties are expected to lead to changes in the position of microwave energy deposition within the liver tissue. The relative permittivity and conductivity are directly taken from [14]. A linear approximation of the dielectric properties is used to estimate the heating rate at temperatures between 37 and 100°C is given as following function:

$$\varepsilon_{r,liver}'(T) = -0.0424T + 47.043 \tag{5}$$

$$\sigma_{liver}(T) = -0.0004T + 1.7381. \tag{6}$$

Microwave energy is emitted from the MCA slot, which connected to the microwave generator. Microwave energy is propagating through the MCA and into the liver tissue from the MCA slot. Where the boundary conditions for analyzing electromagnetic wave propagation are considered as follows:

At the inlet of the MCA, TM wave propagation with input microwave power of 10 W is considered. An axial symmetry boundary is applied at $r = 0$:

$$\vec{E}_r = 0 \tag{7}$$

$$\frac{\partial \vec{E}_z}{\partial r} = 0. \tag{8}$$

Scattering boundary conditions are used along the outer sides of the liver boundaries to prevent reflection artifacts:

$$\hat{n} \times \sqrt{\varepsilon}\vec{E} - \sqrt{\mu}\vec{H}_\varphi = -2\sqrt{\mu}\vec{H}_{\varphi 0} \tag{9}$$

where $\vec{H}_{\varphi 0} = C/Zr$ is the excitation magnetic field.

The H_φ of a spherical wave generated by antenna can be calculated as:

$$\hat{n} \times \left(\nabla \times \vec{H}_\varphi \right) - jk\vec{H}_\varphi = 0. \tag{10}$$

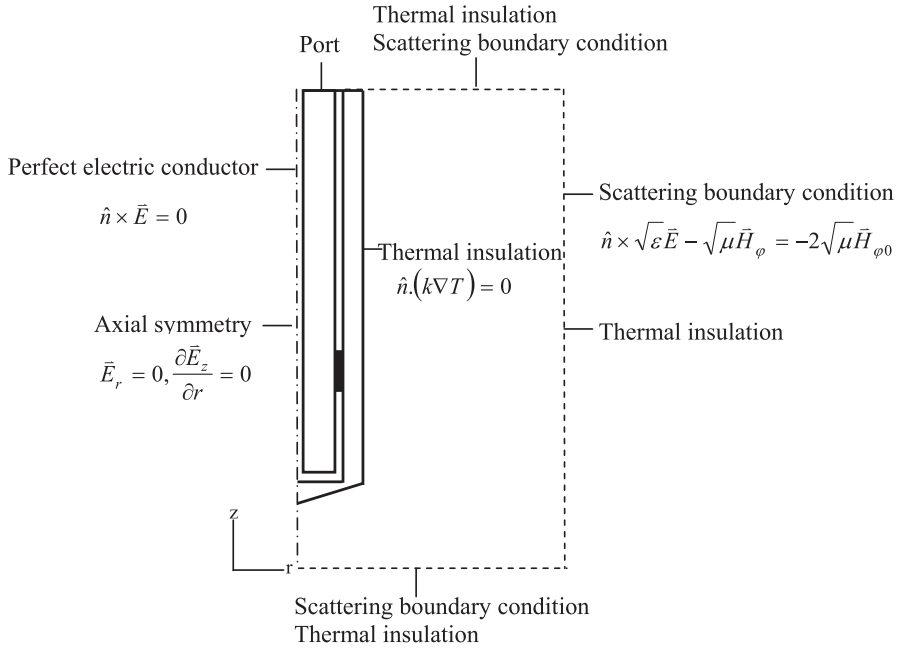

Fig. 3. Boundary conditions for analysis.

For simplicity and to eliminate numerical error, the inner and outer conductors of the antenna are modeled as the perfect electric conductor (PEC) wall:

$$\hat{n} \times \vec{E} = 0 \tag{11}$$

3.2. Heat transfer analysis

Pennes' bioheat equation, introduced by Pennes [15] based on the heat diffusion equation, is a frequency used for analysis of heat transfer in biological tissues (Chua et al. [16], Shih et al. [17] and Wessapan et al. [18]). The transient bioheat equation effectively describes how heat transfer occurs in liver tissue. The equation can be written as:

$$\rho C \frac{\partial T}{\partial t} = \nabla \cdot (k_{th} \nabla T) + \rho_b C_b \omega_b (T_b - T) + Q_{met} + Q_{ext}. \tag{12}$$

Where, the left hand side of Eq. (12) denotes the transient term. The first, second, third and fourth terms on the right hand side of Eq. (12) denote heat conduction, heat dissipation by the blood flow, metabolic heat source and external heat source (heat generation by the electric field), respectively.

One could consider that the PTFE catheter is a thermal insulator and the heat transfer analysis is limited to the liver tissue domain; therefore, thermal properties are only needed for liver tissue and blood. The metabolic heat generation rate of 33,800 W/m^3 [19,20] is used throughout calculation process. The external heat source is equal to the resistive heat generated by the electromagnetic field which can be defined as:

$$Q_{ext} = \frac{1}{2} \sigma_{liver} \left| \vec{E} \right|^2. \tag{13}$$

Where, the electrical properties strongly affect the temperature increase [21]. When microwave propagates in liver tissue, microwave energy is absorbed by liver tissue and converted into internal heat generation which causes the tissue temperature to rise. The SAR represents the electromagnetic power deposited per unit mass in tissue (W/kg) and is defined by:

$$SAR = \frac{\sigma_{liver}}{2\rho} \left| \vec{E} \right|^2. \tag{14}$$

The SAR distribution is widely used for performance evaluation of heating equipment employed in MWA.

Eq. (12) can be rewritten in the form of SAR as

$$\rho C \frac{\partial T}{\partial t} = \nabla \cdot (k_{th} \nabla T) + \rho_b C_b \omega_b (T_b - T) + Q_{met} + \rho SAR. \tag{15}$$

In this study, the temperature dependent properties are considered in calculation procedure. Valvano et al. [22] measured liver tissue thermal conductivity as a function of temperature as shown in following correlation:

$$k_{th}(T) = 0.0012^T + 0.4692 \tag{16}$$

Bioheat transfer processes in living tissues are often influenced by the blood perfusion through the vascular network on the local temperature distribution [23]. When there is a significant difference between the temperature of blood and the tissue through which it flows, convective heat transport will occur, altering the temperatures of both the blood and the tissue. Therefore, an understanding of the heat transfer in living tissue must be accounted for the influence of blood perfusion. Where the blood perfusion rate which depends on temperature can be defined as:

$$\omega_b(T) = 0.000021T + 0.00035 \tag{17}$$

The heat transfer analysis is considered only in the liver tissue domain, which does not include the MCA. The boundaries of the liver tissue are considered as insulating boundary conditions:

$$\hat{n}.(k \nabla T) = 0 \tag{18}$$

Initially, the temperature distribution within the liver tissue is assumed to be uniform:

$$T(t_0) = 37^{\circ}\mathrm{C} \tag{19}$$

4. Calculation procedure

In this study, the FEM is used to analyze the transient problems. The computational scheme is to assemble axisymmetric FE model and compute a local heat generation term by performing an electromagnetic calculation using tissue properties. In order to obtain a good approximation, a fine mesh is specified in the sensitive areas. The coupled equations of electromagnetic wave propagation and bioheat equation is solved by the FEM, which was implemented using COMSOL™ MULTIPHYSICS 3.4, to demonstrate the phenomenon that occurs within the

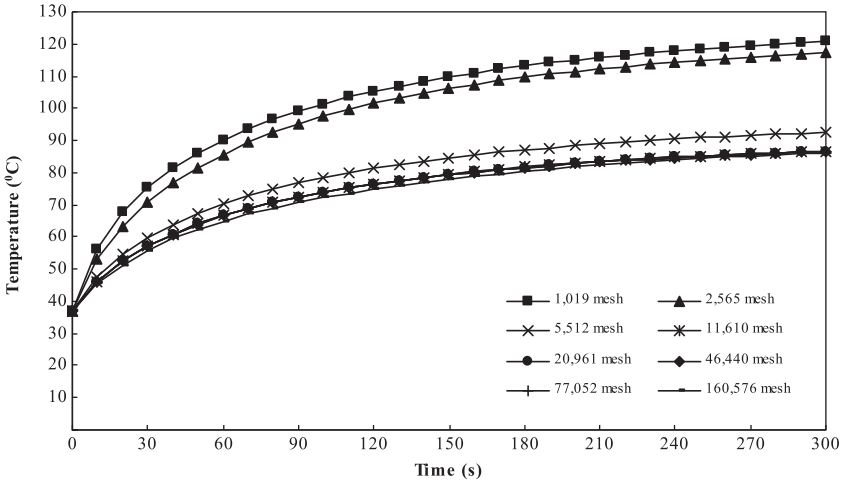

Fig. 4. Relationship between temperature and time from the simulation with the different number of meshes.

Table 3
Computational mesh parameters.

Mesh parameters	Values
Element growth rate	1.3
Maximum element size scaling factor	1
Mesh curvature cut off	0.001
Mesh curvature factor	0.3

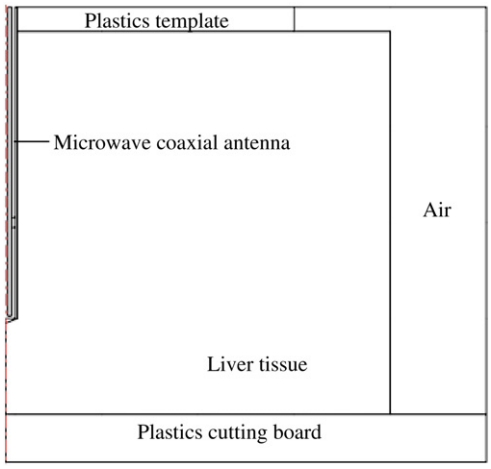

Fig. 5. Geometry of the validation model obtained from the Yang et al. [8].

tissue during MWA. The study employs an implicit time step scheme to solve the electromagnetic wave propagation and temperature distribution. In this study, a time step of 10^{-2} s and 10^{-12} s are used to solve electromagnetic wave propagation equation and bioheat equation, respectively. These are found to be practical to achieve each time step convergence. The temperature distribution has been evaluated by taking into account the SAR due to the electromagnetic field exposure at a particular frequency. Until the steady state is reached, the temperature at each time step is collected.

The axisymmetric FE model is discretized using triangular element, and the Lagrange quadratic is used to approximate microwave power absorbed, SAR and temperature distribution variation across each element. The convergence test of the frequency of 2.45 GHz is carried out to identify the suitable numbers of element required. The number of elements where solution is independent of mesh density is found to be 11,610. The convergence curve resulting from the convergence test is shown in Fig. 4. Where Fig. 4 shows the relationship between temperature and time from simulations at a critically sensitive point, 2.5 mm away from the antenna and longitudinally aligned with the single slot MCA, for different meshes. Computational mesh parameters shown in Table 3.

5. Results and discussion

5.1. Verification of the model

To verify the accuracy of the presented mathematical model of MWA, the resulting data with single slot MCA is validated against the simulation results, obtained by Yang et al. [8]. Fig. 5 shows the geometry of the validation model. In the validation case, the microwave power of 75 W with frequency of 2.45 GHz and the initial liver tissue temperature of 8 °C are selected. The radius of single slot MCA is 1.25 mm. It is inserted 20 mm deep into liver tissue. The axially symmetrical model is used to analyze the MWA process and the heating duration is 150 s.

Fig. 6 shows the validation results of the liver tissue temperature, with respect to the heating time of MWA at the positions of 4.5 mm and 9.5 mm away from the single slot MCA. It is found that the simulated results are corresponded closely with the Yang et al. [8]. Table 4 clearly shows a good agreement of the tissue temperature between the present solution and that of Yang et al. [8]. Certain amounts of mismatch between the simulated results and the results obtained from Yang et al. [8] have been identified for some dielectric and thermal properties. In addition, the error involved in the simulation is caused by the numerical scheme.

5.2. Comparison of single slot MCA and double slot MCA

5.2.1. Microwave power absorbed

Fig. 7 shows the computer-simulated results of microwave power absorbed in liver tissues base on a frequency of 2.45 GHz and microwave power of 10 W. Fig. 7(a) shows the microwave power absorbed in liver tissues in case using single slot MCA and Fig. 7(b) in case using double slot MCA for durations of 30 s, 120 s, and 300 s. The figures illustrate the volume heating effect expected from MWA. Microwaves power emitted from the MCA propagates through the liver tissue, which is converted to heat by dielectric heating. According to the results, in both cases, the microwave power absorbed distribution is a near ellipsoidal around the slot and its highest values in the vicinity of the slot MCA and decreases with the distance. Where the comparison of the microwave power absorbed between in case using single slot MCA and using double slot MCA, it is found that

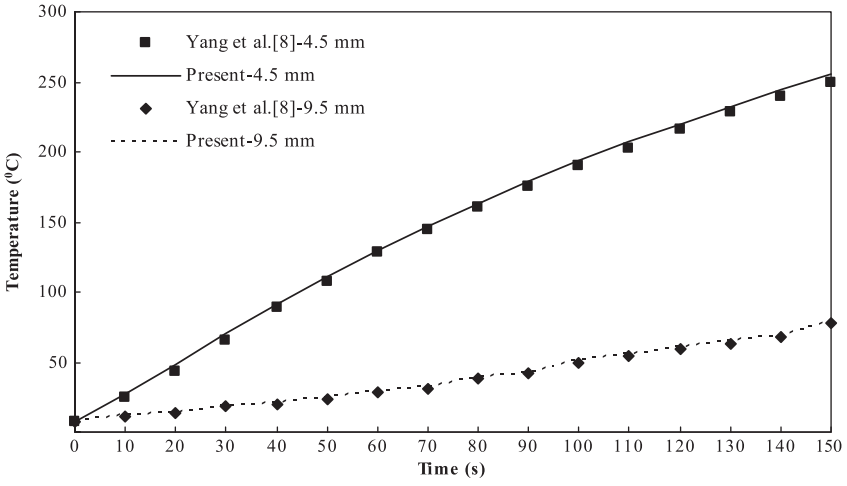

Fig. 6. The validation results of the liver tissue temperature, against Yang et al. [8].

Table 4
Comparison of the results obtained in the present study with those of Yang et al. [8].

	Present	Yang et al. [8]	Difference (%)
4.5 mm	11.03	6.34	3.1
9.5 mm	48.53	45.13	3.4

double slot MCA generates a wider microwave power absorbed distribution pattern in liver tissue than a standard single slot MCA.

5.2.2. SAR distribution

Fig. 8 shows the comparison of SAR distribution between case of single slot MCA and double slot MCA along a line parallel to the MCA axis with $r = 2.5$ mm which base on a frequency of 2.45 GHz, microwave power of 10 W and heating time of 300 s. In both cases, the SAR distributions gradually increase along the longitudinal axis of the MCA to a maximum at the slot exit. In case of single slot MCA, the peak SAR value obtained for 10 W of microwave power is 2.63 kW/kg at the insertion depth of approximately 64 mm. While in case of double slot MCA, the peak SAR value of 2.37 kW/kg is obtained at the insertion depth approximately of 58.3 mm close to the upper slot position. After that the SAR values quickly decreases and have the lowest value at the insertion depth of 80 mm. A less than ten percent difference between the two cases can be obtained. It is found that the variation of SAR values in the liver tissue is due to the antenna type and the insertion depth.

The results indicate that the SAR value of single slot MCA is higher than that of double slot MCA in almost every position, except the area between the insertion depths of 57–58 mm which is the position of the upper slot of double slot MCA. In addition, the SAR distribution in case of using single slot MCA is higher than that found in the case of using double slot MCA, which corresponds to a higher microwave power absorbed, as shown in Fig. 7. This is because higher attenuation of the microwave reduces the contributions of propagated waves as they propagate through the double slot MCA. However, there is no

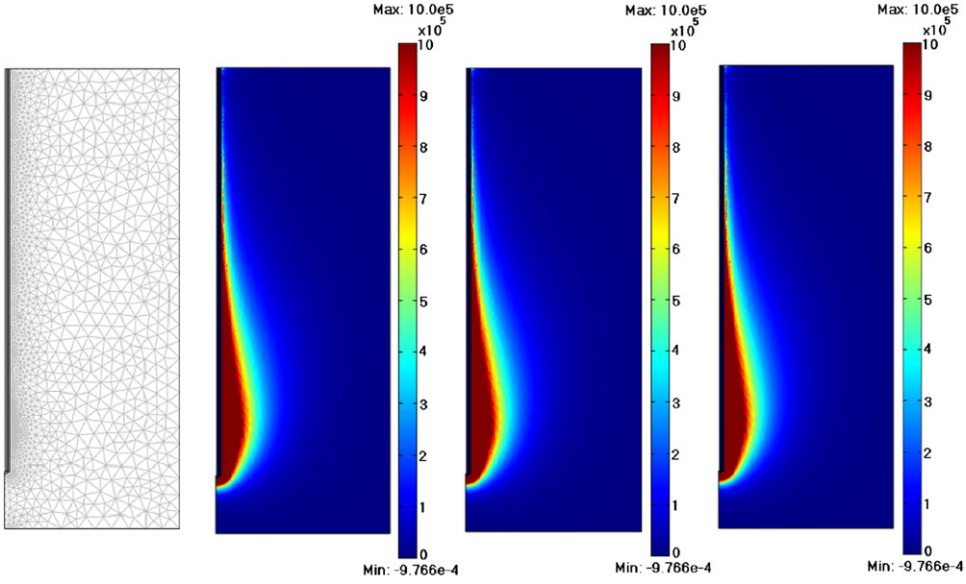

(a) single slot MCA

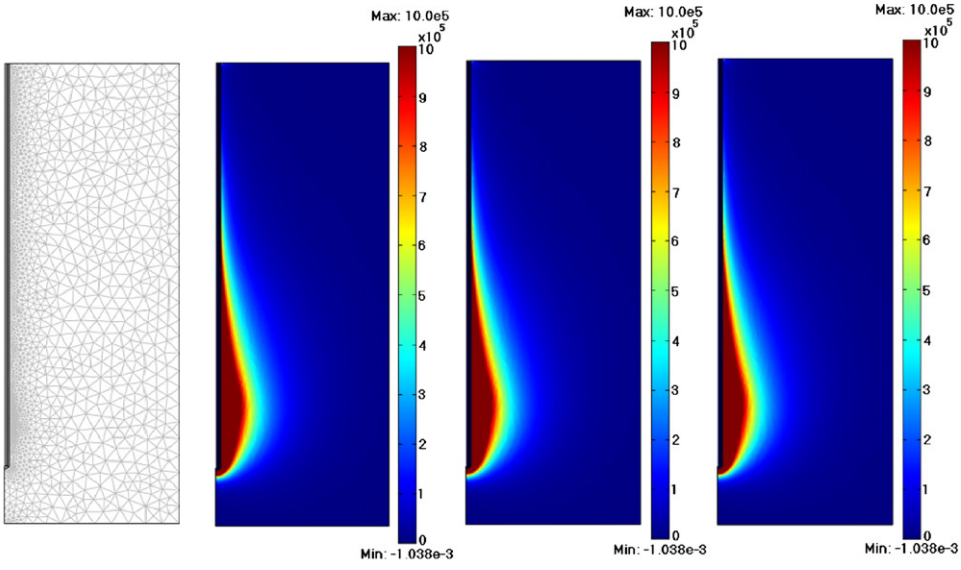

(b) double slot MCA

Fig. 7. The microwave power absorbed in liver tissue for various heating times 30 s, 120 s and 300 s, respectively (the scale is cut off at $10^6 W/m^3$) (W/m^3).

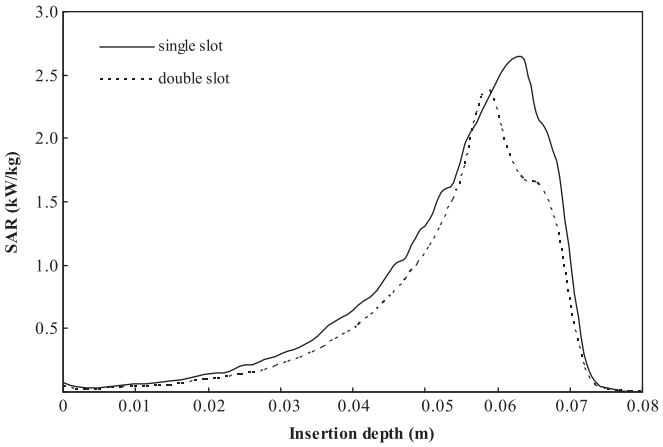

Fig. 8. Comparison of SAR distribution between in case of using single slot MCA and double slot MCA.

clear difference between these two MCA models, due to the low microwave power input that has been used in this study.

5.2.3. Temperature distribution

The basic principle of MWA is to apply microwave power to the liver tissue through the MCA. The microwave energy is absorbed by the liver tissue and heats it. Liver tissue is destroyed after it is heated to a high enough temperature for a sufficiently long time. The ultimate goal of ablation technology, considering MWA, is to kill the liver cancer cells, while effectively preserving the healthy liver tissue. Fig. 9 shows the simulated results of temperature distribution in liver tissues based on a frequency of 2.45 GHz and microwave power of 10 W. The temperature distributions for durations of 30 s, 120 s, and 300 s shown in Fig. 9(a) and (b) are obtained from the single slot and double slot MCA, respectively. In both cases, the temperature distribution is near ellipsoidal distribution around the slot and its highest values in the vicinity of the slot MCA and decreases with the distance which corresponds to the microwave power absorbed (as

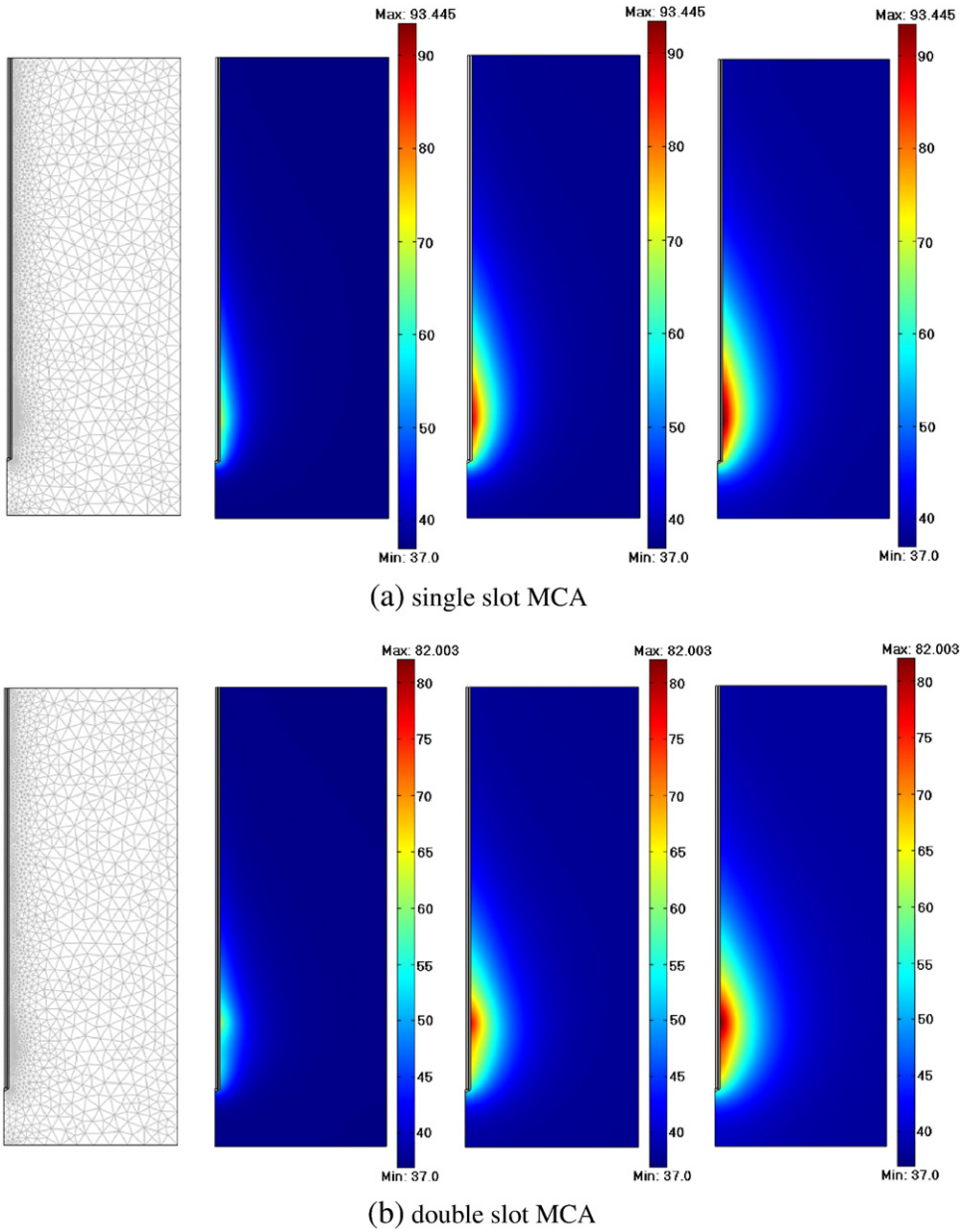

Fig. 9. The temperature distribution in liver tissue for various heating times 30 s, 120 s and 300 s, respectively (°C).

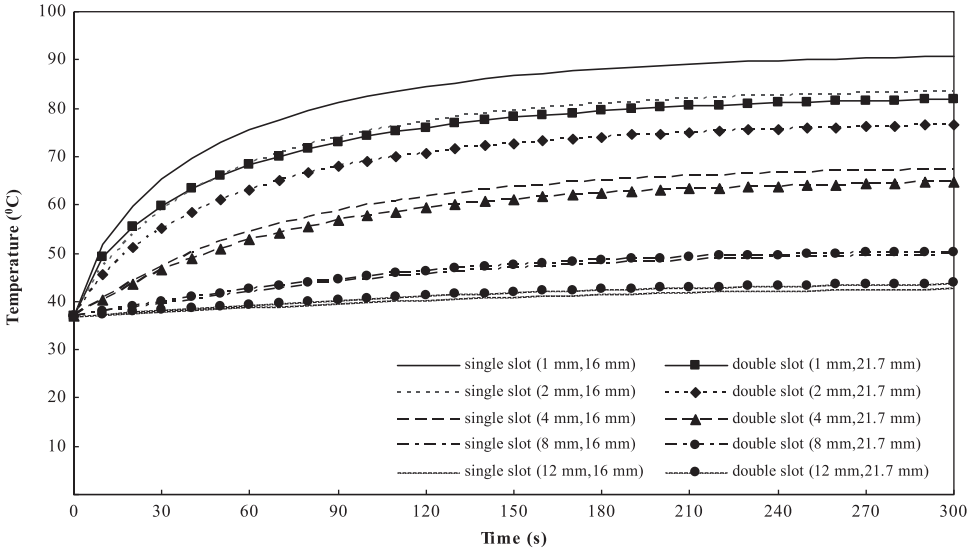

Fig. 10. Comparison of the five position temperature curves at level of the upper slot exit in case of using single slot MCA ($z=16$ mm) and double slot MCA ($z=21.7$ mm) versus time.

shown in Fig. 7). In addition, temperature distribution increases with increasing time. This is because the microwave power absorbed within the liver tissue attenuates, owing to energy absorption, and thereafter the absorbed energy is converted into thermal energy, which increases the liver temperature. The maximum temperature within the liver tissue at t = 300 s are 93.445°C and 82.003°C for the single slot and double slot MCA, respectively.

Fig. 10 shows the comparison of the five position temperature curves at level of the upper slot exit in case of using single slot MCA ($z=16$ mm) and double slot MCA ($z=21.7$ mm) versus time. The results of both cases show similar trends of temperature distribution that is the temperature increases with increasing time. At the position of 1 mm and 4 mm from the MCA, the results indicate that the temperature of single slot MCA is higher than that case of double slot MCA, while temperature of double slot MCA is higher than that case of single slot MCA specified at the position of 8 mm and 12 mm. Moreover, the temperatures differences for the two cases are 9.77% at the position of 1 mm, 8.30% at the position of 2 mm, 3.98% at the position of 4 mm, 1.27% at the position of 8 mm and 2.28% at the position of 12 mm, respectively.

Fig. 11 shows the comparison of temperature distribution between in case of using single slot MCA and double slot MCA along a line parallel to the MCA axis with $r=2.5$ mm based on a frequency of 2.45 GHz and microwave power of 10 W at a heating time of 300 s.

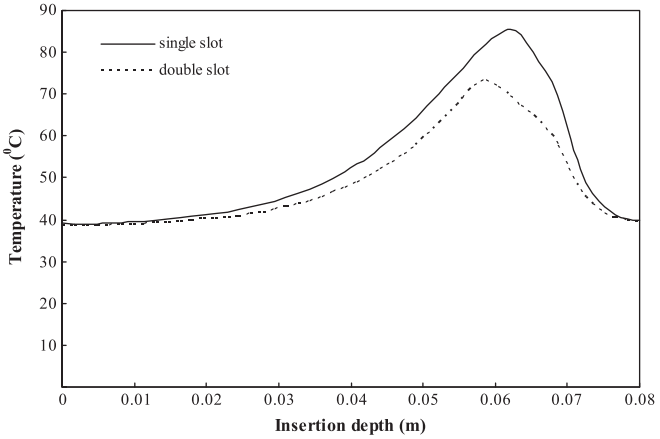

Fig. 11. Comparison of temperature distribution between in case of using single slot MCA and double slot MCA.

The results of both cases show similar trends of SAR distribution as shown in Fig. 8 (which correspond to Eq. (14)). In both cases, the temperature distributions gradually increase from the insertion depth of 10 mm to the slot position. The highest temperature values are obtained at slot position (the insertion depth of approximately 64 mm or $z=16$ mm) is 85.52 °C for using the single slot MCA. While using the double slot MCA, the highest temperature values of 73.31 °C are obtained at the insertion depth of approximately 58.3 mm ($z=21.7$ mm) at the upper slot position. There is a 14.28% difference between the highest temperature values of the two cases. After that the values quickly decreases and have the lowest value at insertion depth of 80 mm. It is found that the temperature distribution in the liver tissue is different due to the antenna type and the insertion depth position which corresponds to SAR distribution.

6. Conclusion

This work presents an analysis of electromagnetic wave propagation with coupled to heat transfer for liver MWA using single and double slot MCA, with the objectives to approach the appropriate applicator for a given treatment area. In this work, single and double slot MCA for interstitial MWA in liver is evaluated in order to compare their effects on the microwave power absorbed, SAR distribution and temperature distribution in the liver tissue. It is found that the microwave power absorbed, SAR distribution and temperature distribution in the liver tissue is strongly dependent on the number of MCA slot. The highest SAR and temperature values obtained for the liver tissue in case of single MCA are found to be higher than those of the double slot MCA. However, the double slot MCA having a larger ablation area of high temperature than that of the single slot MCA. It is found that, the shape and size of the destructed area can be varied by adjusting the configuration and antenna design, resulting in no damage to the surrounding tissues.

In next step of research, the formulation of 3D modeling for approaching realistic liver tissue will be performed. Current work has already done is to simulate the MWA in tissue where this tissue is modeled as a porous media base. During this MWA process, the phase transition in porous tissue domain will be considered in order to approach realistic phenomena in practical work [24].

Acknowledgments

This work was financially supported by the Thailand Research Fund (TRF) and Thammasat University.

References

[1] J.F. McGahan, G.D. Dodd Iii, Radiofrequency ablation of the liver: current status, American Journal of Roentgenology 176 (1) (2001) 3–16.
[2] W.Y. Lau, T.W.T. Leung, S.C.H. Yu, Percutaneous local ablative therapy for hepatocellular carcinoma: a review and look into the future, Annals of Surgery 237 (2) (2003) 171–179.
[3] Ablative techniques (percutaneous) thermal ablative techniques, in: T.J. Vogl, T.K. Helmberger, M.G. Mack, M.F. Reiser (Eds.), Percutaneous Tumor Ablation in Medical Radiology, Springer, Berlin, Germany, 2008, pp. 7–32.
[4] R.J. Schweikert, R.G. Keanini, A finite element and order of magnitude analysis of cryosurgery in the lung, International Communications in Heat and Mass Transfer 26 (1) (1999) 1–12.
[5] S.B. Chinn, F.T. Lee Jr., G.D. Kennedy, et al., Effect of vascular occlusion on radiofrequency ablation of the liver: results in a porcine model, American Journal of Roentgenology 176 (3) (2001) 789–795.
[6] S. Garrean, J. Hering, A. Saied, et al., Ultrasound monitoring of a novel microwave ablation (MWA) device in porcine liver: lessons learned and phenomena observed on ablative effects near major intrahepatic vessels, Journal of Gastrointestinal Surgery 13 (2) (2009) 334–340.
[7] K. Saito, Y. Hayashi, H. Yoshimura, K. Ito, Heating characteristics of array applicator composed of two coaxial-slot antennas for microwave coagulation therapy, IEEE Transactions on Microwave Theory and Techniques 48 (2000) 1800–1806 (1 PART 1).
[8] D. Yang, M. Converse, D. Mahvi, Expanding the bioheat equation to include tissue internal water evaporation during heating, IEEE Transactions on Biomedical Engineering 54 (8) (2007) 1382–1388.
[9] M. Cepeda, A. Vera, L. Leija, et al., Coaxial double slot antenna design for interstitial hyperthermia in muscle using a finite element computer modeling, IEEE International Instrumentation and Measurement Technology Conference I2MTC (2008) 961–963.
[10] J.P. McGahan, J.M. Brock, H. Tesluk, W.Z. Gu, P. Schneider, P.D. Browing, Hepatic ablation with use of radio-frequency electrocautery in the animal model, Journal of Vascular and Interventional Radiology : JVIR 3 (2) (1992) 291–297.
[11] J.M. Bertram, D. Yang, M.C. Converse, Antenna design for microwave hepatic ablation using an axisymmetric electromagnetic model, Biomedical Engineering Online 5 (2006).
[12] D. Yang, J.M. Bertram, M.C. Converse, et al., A floating sleeve antenna yields localized hepatic microwave ablation, IEEE Transactions on Biomedical Engineering 53 (3) (2006) 533–537.
[13] S. Jacobsen, P.R. Stauffer, Can we settle with single-band radiometric temperature monitoring during hyperthermia treatment of chestwall recurrence of breast cancer using a dual-mode transceiving applicator? Physics in Medicine and Biology 52 (4) (2007) 911–928.
[14] C.L. Brace, Temperature-dependent dielectric properties of liver tissue measured during thermal ablation: toward an improved numerical model, Conference proceedings: Annual International Conference of the IEEE Engineering in Medicine and Biology Society, IEEE Engineering in Medicine and Biology Society (2008) 230–233.
[15] H.H. Pennes, Analysis of tissue and arterial blood temperatures in the resting human forearm, Journal of Applied Physiology 85 (1) (1998) 5–34.
[16] K.J. Chua, J.C. Ho, S.K. Chou, M.R. Islam, On the study of the temperature distribution within a human eye subjected to a laser source, International Communications in Heat and Mass Transfer 32 (8) (2005) 1057–1065.
[17] T.C. Shih, H.L. Liu, A.T.L. Horng, Cooling effect of thermally significant blood vessels in perfused tumor tissue during thermal therapy, International Communications in Heat and Mass Transfer 33 (2) (2006) 135–141.
[18] T. Wessapan, S. Srisawatdhisukul, P. Rattanadecho, The effects of dielectric shield on specific absorption rate and heat transfer in the human body exposed to leakage microwave energy, International Communications in Heat and Mass Transfer 38 (2) (2011) 255–262.
[19] J. Lienhard, A Heat Transfer Textbook, Phlogiston, Lexington, MA, 2005.
[20] Y. Rabin, A. Shitzer, Numerical solution of the multidimensional freezing problem during cryosurgery, Journal of Biomechanical Engineering 120 (1) (1998) 32–37.
[21] M. Fujimoto, A. Hirata, J. Wang, et al., FDTD-derived correlation of maximum temperature increase and peak SAR in child and adult head models due to dipole antenna, IEEE Transactions on Electromagnetic Compatibility 48 (1) (2006) 240–247.
[22] J.W. Valvano, J.R. Cochran, K.R. Diller, Thermal conductivity and diffusivity of biomaterials measured with self-heated thermistors, International Journal of Thermophysics 6 (3) (1985) 301–311.
[23] J. Shi, Z. Chen, M. Shi, Simulation of heat transfer of biological tissue during cryosurgery based on vascular trees, Applied Thermal Engineering 29 (8–9) (2009) 1792–1798.
[24] P. Ratanadecho, K. Aoki, M. Akahori, Influence of irradiation time, particle sizes, and initial moisture content during microwave drying of multi-layered capillary porous materials, Journal of Heat Transfer 124 (1) (2002) 151–161.